Particle Shape Effects on Flowability of Powder Mixtures

Edward Wyburn[1], Benjy Marks[1], François Guillard[1], Pierre Rognon[1], Itai Einav[1,2]

[1]Particles and Grains Laboratory, School of Civil Engineering, The University of Sydney, Sydney, New South Wales 2006, Australia

[2]Department of Civil, Environmental & Geomatic Engineering, Faculty of Engineering Science, University College London, London WC1E 6BT, UK

ABSTRACT Particle shape has a significant effect on granular rheology. Often in experiments and simulations spherical particles are used for simplicity, however it is rare that these shapes are actually present within a real flow. The influence of particle size in regards to flowability has been studied extensively, with the diameter of circular or spherical objects strongly controlling the resulting behaviour. An increase in the elongation of grains has been shown to slow the flow, yet the effect of mixtures of particle shapes in differing proportions has yet to be characterised rigorously. To study this phenomenon we place a single intruder particle within a simple shear configuration to study the effect on the rheology. We find that particle shape strongly influences the flow behaviour. This could lead to new opportunities to improve flowability in various applications.

1. INTRODUCTION

Granular flows are one of the most ubiquitous phenomenon in both the natural and industrial worlds, yet much of their nature remains undiscovered. Granular rheology seeks to capture behaviour all the way from mostly liquid flows, such as concrete, to completely dry flows, such as glass beads. Additives and admixtures have been shown to change the flowing properties of substances, whether it be corn flour to thicken a broth, additives to reduce the slump of concrete, polymers placed in a turbulent non-newtownian fluid to reduce drag [1], or nanoparticles improving the flowability of cohesive powders through mechanisms which reduce both clumping the angle of repose [2]. The choice of admixture and the mechanism by which it operates is system dependent.

It comes as no surprise that particle shape will have an effect on the behaviour of granular flows. Most simulations and fundamental experiments use spheres or circles due to the simplicity of those shapes [3]. Studies have been performed on the effect of systems consisting of entirely irregularly shaped particles such as [4,5], as well as intruders pulled through a mass of grains [6] or placing obstacles within flows [7,8], yet the effect of placing relatively few intruder particles within a free flowing mass of regular particles remains currently unknown. A comprehensive study on how shape of intruders affects the bulk flow rate of a granular material is lacking.

In this paper preliminary results are presented which look at the behaviour of a single 2D teardrop shaped particle within our Stadium Shear apparatus (which is discussed in the next section). The information presented has been gathered at one belt velocity and confining pressure. The Stadium Shear device has been both used for experiments [9,10,11] and simulated [12], as well as recently simulated using entirely irregular shaped particles [5]. The device is similar to the "$1\gamma 2\epsilon$" apparatus [13] which also imparts shear on 2D analogues, yet a distinct limitation of the $1\gamma 2\epsilon$ is that it is only able to deform the material a limited amount. A significant advantage of the stadium shear device is that it allows for infinite deformation at constant velocity.

2. METHOD

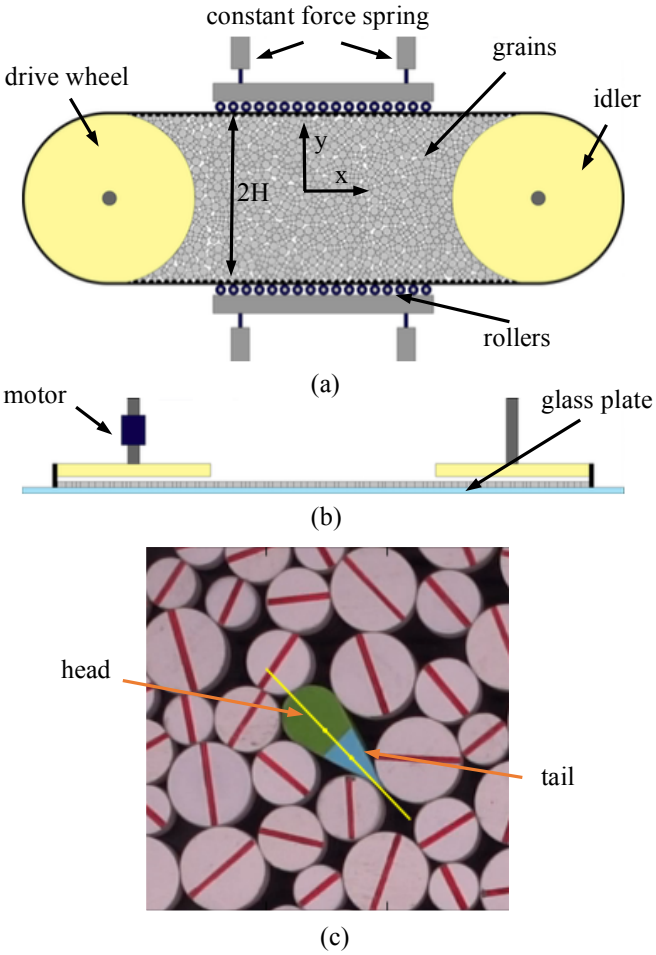

Figure 1 Stadium Shear Device [11]

The Stadium Shear apparatus is shown in Figure 1. Part (a) of the image is a top view which shows the granular assembly which will be deformed, the belt which travels around the outside to impart shear, as well as the rollers attached with constant force springs to alter the external pressure placed upon the system and control the inertial number. The two spindles around which the belt is run has one driving and one idle. Part (b) shows a side view of the apparatus. Note that grains are able to travel underneath the spindles, which coupled with the stadium shape allows for the infinite shear of the 2D grain analogues. A picture of the intruder and some surrounding grains is presented in part (c). The yellow line is drawn on to show the orientation of the particle, with one dot at the centroid of the teardrop and one at the centroid of the blue area. The other grains are 10mm high nylon cylinders, with three different diameters (12, 15 and 20mm) in order to avoid crystalisation. In addition to these cylinders, the single 3D printed PLA teardrop shaped intruder particle is 15mm in diameter, 10mm in height and with a longer tail (32mm in total length).

To quantify the motion of the full field including the intruder, particle tracking velocimetry (PTV) has been performed on videos of the flow. The videos were captured in 1920x1080 resolution at a nominal frame rate of 60fps – this frame rate allowed for movement of less than $1/4^{th}$ of a grain diameter between frames which allows for tracking individual grains. The images were binarised using a filter, and on the black and white image a distance transform and threshold was applied to find each individual object. The intruder particle is a different colour, so it was identified by looking for the largest object which passed separate colour thresholds. The tail of the intruder has been coloured separately using tape so that the rotation of the object can be easily identified.

In order to gain significant statistics on the intruder particle, since there has only been one placed within the system for these tests, the device had to be sheared for a long time to get significant data – much more than was found to be required to retrieve a smooth field for the surrounding grains. To get continuum data on the full field from the

discrete measurements taken for the surrounding grains, coarse graining [14] using a modified 2D lucy function [10] has been applied to the data gathered.

3. RESULTS

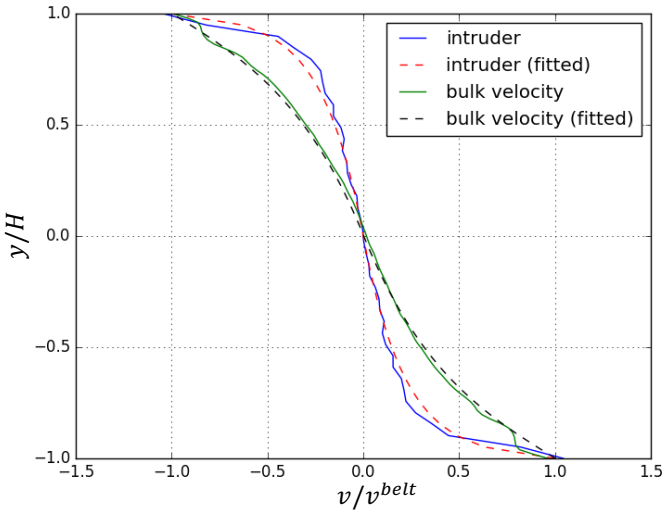

Figure 2 Normalised Velocity Profile

Within Figure 2, the unbroken lines denote experimental data and the dashed lines denote best fits using the eddy viscosity model, which is discussed later. A striking feature of the velocity profile within the experiment is the non-linear but symmetric 's' shaped profile. The expectation would be at first glance that a linear profile is present within the flow, as is found within a simple shear configuration, but due to the non-linearity of granular materials and the intrinsic length scales between the two opposing flows the behaviour becomes more complicated. This 's' profile has been found in experiments [9,10,11] and also from numerical simulations on the same configuration [5,12]. There exists a kink within the experimental bulk velocity profile at approximately $y/H = \pm 0.9$ which is caused by the entrainment of grains within the asperities of the belt. Also included on this graph is the velocity profile of the intruder. The intruder's profile has been created from binning the velocity values by their distance from the centre. There exist significantly fewer data points gathered for the intruder which introduces the jagged shape of its profile. Due to the symmetric nature of the system, the information for the intruder has been mirrored in order to increase the number of data points for each position on the graph. Without mirroring these values the profile was still relatively symmetric and s-shaped but more jagged. Coarse graining was not applied to the intruder due to its non-symmetric shape and subsequently an appropriate choice of function remains a concern.

It is clear from Figure 2 that the intruder is systematically slower than the surrounding grains – except for when the intruder gets stuck within the asperities of the belt and is pulled at the belt velocity. In order to verify the effect of the intruder's shape, a future study varying the properties (total length, head diameter) of the particle will be conducted. It remains unclear how much of this behaviour is due to size effects of the particle (the inertial number of the particle itself being higher, which is known to affect the system's friction most notably with the $\mu(I)$ rheology [3,15]), or an increased friction coefficient between the 3D printed PLA and the glass. The friction coefficient between the nylon cylinders and the glass is very small, measured to be 0.072, and while the interface between the intruder and glass is smooth it is likely to be higher than this value. In order to remove the interference of the materials an entire new set of particles will be cast in a photoelastic material – which will have the added benefit of allowing for the stress field to be observed.

$$\dot{\gamma}(y) = \frac{aV^{belt}}{d\sinh^{-1}(aH/d)}\left(1 + a^2\left(\frac{H-|y|}{d}\right)^2\right)^{-1/2} \quad (1)$$

A concise explanation of the velocity of the intruder is described by an eddy viscosity model, which has been presented by Miller et al. [9]. The shear rate produced by this model is presented as Equation (1). This shear rate has been integrated to produce the fitted velocity profiles found in Figure 2. The immediate result of this fitting is that the numerical constant related the correlation length increases from a = 0.46 for the surrounding particles to a = 6.32 for the intruder. While there exists some uncertainty as to what exactly the equivalent diameter within

Equation (1) of the intruder shape should be, the value of a is roughly linearly proportional to the diameter in this equation within the current range and as such the factor of ~14 between the two fits will be more robust than any reasonable choice of diameter. The value of $a = 6.32$ is very large, and since it is significantly larger than unity (which would mean that a particle in the centre diffuses momentum all the way to the wall), it would suggest that when considering the intruder it would be forming correlated structures of sizes much larger than the system itself and be breaking the eddies created by the mass of cylinders.

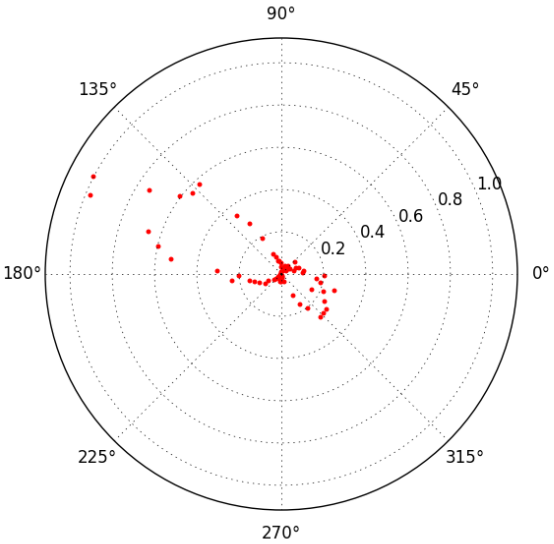

Figure 3 Angle Tendency of Intruder

Figure 3 shows the tendency of the particle to orient itself at certain angles. This data was gathered from the centroids of the teardrop and is denoted by the yellow line in Figure (1)(c). The angle in Figure 3 relates relates to the orientation of the particle while the radial distance is a histogram normalised to the largest count obtained. This angle has been taken relative to the belt motion in the half of the device that the grain is sitting. Since the data is mirrored a clockwise rotation in the bottom half of the experiment is the same as a counter-clockwise rotation in the top half of the media. Angles between 0° and 180° in this graph mean that the tail is oriented towards the belt, and between 180° and 360° mean that the head is oriented towards the belt. On this graph, an angle of 0° is "head first" motion and an angle of 180° is "tail first" motion. This graph shows the strong tendency of the intruder to progress tail first, or be "wedging" between the cylindrical grains. For the intruder particle considered, the angle made between the two sides of the tail is approximately 36°, or each side being 18° from the horizontal, which doesn't line up with the ~20-30° preferred orientation of the particle. Due to this skew in the frequency of these events this graph can be read as the preferred orientation of the particle is the tail is pushed by the more swiftly moving particles while the head sits within the slower ones. To see how this preferred orientation is altered by the length and angle of the tail will require a further parametric study.

Data within Figure 3 has been not been taken at points closest to the belt (where entrainment occurs and the particle is kept at the same angle for a large period of time) or near where the intruder crosses the centre since the orientation of the particle relative to the flow becomes poorly defined.

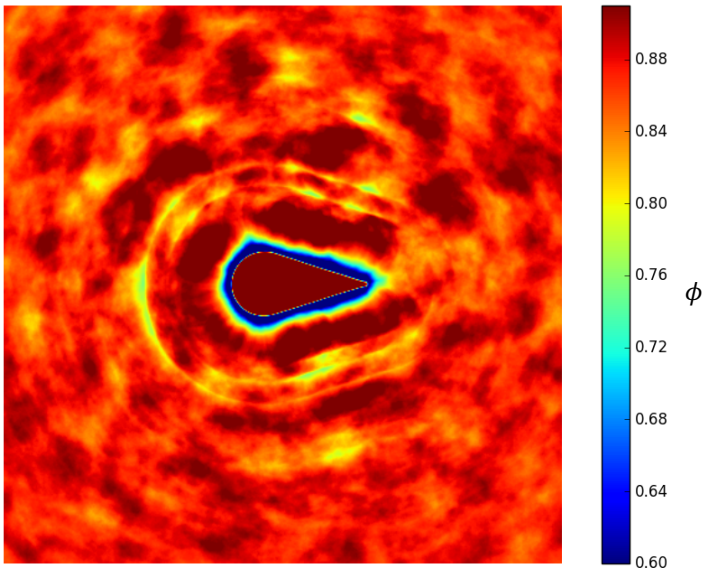

Figure 4 Density Around Intruder

In Figure 4, the density profile (time-averaged solid fraction) of the area around the intruder is presented. All images that contained the particle a sufficient distance to the boundaries have been averaged to produce this figure, and have been rotated such that the intruder is at the same orientation for each one. As such the probability that the grain will be present within the image is 100%. The halo of lower density surrounding the intruder particle is due to the small contact area between particles and the intruder. Three streaks of lower density surround the intruder which represent the diameters of the grains within the device. Interestingly the regions of highest solid fraction are those immediately surrounding the particle. There appears to be a wake after the tail end of somewhat lower density, such as that found in an intruder pulled through a mass of smaller particles [6] – however this is in contrast with how the particle has a tendency to wedge, and a much larger field of view would be required to view any possible wake properly.

4. CONCLUSIONS

We have shown that the intruder particle behaves differently to the rest of the particles. This was accentuated by its slower velocity profile, which was also well captured by the eddy viscosity model. Whether the difference between the profiles is purely a function of the shape, or has more to do with the size, inertial number and friction coefficient of the intruder will have to be explored with a systematic study of these variables. Of particular interest for future study will be the preferred angle of the intruder and what factors contribute to this phenomenon.

5. ACKNOWLEDGEMENTS

The authors would like to acknowledge the financial support provided by the Australian Research Council through Discovery Project DP130101291. The authors would also like to thank Garry Towell and Ross Barker for their continued support, as well as Tom Miller for his pioneering work.

6. NOMENCLATURE

(All values used within figures have been normalised: velocities relevant to the belt, and distances relevant to the half height of the experiment. Data was measured in pixels and pixels/frame before non-dimensionalisation)

$\dot{\gamma}$	Shear rate, s^{-1}
y	distance from centre of experiment towards belt, mm
V	Velocity of particle(s), mm/s
V^{belt}	Belt velocity, mm/s
H	Half width of system, i.e. $-H \leq y \leq H$, mm
d	Average grain diameter, mm
ϕ	Time-averaged solid fraction, dimensionless

7. REFERENCES

[1] Den Toonder, J. M. J., Hulsen, M. A., Kuiken, G. D. C., & Nieuwstadt, F. T. M. (1997). Drag reduction by polymer additives in a turbulent pipe flow: numerical and laboratory experiments. *Journal of Fluid Mechanics*, *337*, 193-231.

[2] Tomas, J., & Kleinschmidt, S. (2009). Improvement of flowability of fine cohesive powders by flow additives. *Chemical engineering & technology*, *32*(10), 1470.

[3] GDR MiDi (2004). On dense granular flows. *The European Physical Journal E*, *14*(4), 341-365.

[4] Lumay, G., Boschini, F., Traina, K., Bontempi, S., Remy, J. C., Cloots, R., & Vandewalle, N. (2012). Measuring the flowing properties of powders and grains. *Powder Technology*, *224*, 19-27.

[5] Jerves, A. X., Kawamoto, R. Y., & Andrade, J. E. (2015). Effects of grain morphology on critical state: a computational analysis. *Acta Geotechnica*, 1-11.

[6] Seguin, A., Coulais, C., Martinez, F., Bertho, Y., & Gondret, P. (2016). Local rheological measurements in the granular flow around an intruder. Physical Review E, 93(1), 012904.

[7] Gray, J. M. N. T., Tai, Y. C., & Noelle, S. (2003). Shock waves, dead zones and particle-free regions in rapid granular free-surface flows. *Journal of Fluid Mechanics*, *491*, 161-181.

[8] Tüzün, U., & Nedderman, R. M. (1985). Gravity flow of granular materials round obstacles—I: Investigation of the effects of inserts on flow patterns inside a silo. *Chemical engineering science*, *40*(3), 325-336.

[9] Miller, T., Rognon, P., Metzger, B., & Einav, I. (2013). Eddy viscosity in dense granular flows. *Physical review letters*, *111*(5), 058002.

[10] Miller, T. (2014). The kinematics of dense granular materials under indefinite plane-shear. PhD thesis, School of Civil Engineering, The University of Sydney.

[11] Rognon, P., Miller, T., & Einav, I. (2015). A circulation-based method for detecting vortices in granular materials. *Granular Matter*, *17*(2), 177-188.

[12] Rognon, P. G., Miller, T., Metzger, B., & Einav, I. (2015). Long-range wall perturbations in dense granular flows. *Journal of Fluid Mechanics*, *764*, 171-192.

[13] Calvetti, F., Combe, G., & Lanier, J. (1997). Experimental micromechanical analysis of a 2D granular material: relation between structure evolution and loading path. *Mechanics of Cohesive-frictional Materials*, *2*(2), 121-163.

[14] Weinhart, T., Thornton, A. R., Luding, S., & Bokhove, O. (2012). From discrete particles to continuum fields near a boundary. *Granular Matter*, *14*(2), 289-294.

[15] Jop, P., Forterre, Y., & Pouliquen, O. (2006). A constitutive law for dense granular flows. *Nature*, *441*(7094), 727-730.